Small-Size Blockage Propagation Modeling at 28 GHz for mmWave Communications Systems

Small-Size Blockage Propagation Modeling at 28 GHz for mmWave Communications Systems

Fahd Alsaleem, *Member, IEEE*, John S. Thompson, *Fellow, IEEE*, David I. Laurenson, *Member, IEEE*, Cristian A Alistarh, *Member, IEEE*, and Symon K. Podilchak, *Member, IEEE*

***Abstract*—The short wavelength of the mmWave frequency band suggests that even narrow-width blockers affect the mmWave signal strength. There is a lack of literature investigating the effect of small-sized blockages. In this study, we present new measurement results for five metallic objects, mimicking objects indoors or in the street, where the obtained resulting loss is in the range of 10-30 dB. Based on these new results, the knife-edge diffraction blockage model that is provided by the third-generation partnership project (3GPP) standards body, in general, fails to replicate the results. Thus, we investigate the suitability of the enhanced knife-edge diffraction blockage model, called the mmMAGIC blockage model, for these blockers, which generally works well in capturing the measured attenuations.**

***Index Terms*—mmWave, High frequency, Blockage, Knife-edge diffraction KED, Road signs, Directional Antenna Propagation**

I. Introduction

THE mmWave band shows high sensitivity to blockage attenuation, which is one of the main challenges for communication at these frequencies. Any object crossing the line of sight (LOS) path between the transmitter and the receiver will induce an attenuation that could severely affect the signal strength [1]. Understanding the behavior of the blockage effect is important for the design of beamforming techniques for future mmWave systems [2]–[4]. Human blockage, as an example, typically causes signal attenuation of 20-25 dB [5]. While the effect of human blockage has been well-investigated in the literature over the past few years, the impact of blockers with narrower width in the range of few wave-lengths requires further investigations. Considering carrier frequencies around 28 GHz, the use of "small object or blockage" terminology through this paper means blockers with a narrow width, i.e., in the range of 10 cm up to about 33 cm, which is less than the average shoulder-width of a human body. Examples of outdoor blockage types include road signs, lampposts, and traffic lights, while indoor blocker types include small pieces of furniture such as chairs, small tables, or a personal computer screen.

Diffraction theories have been widely used to model the blockage effects, such as the geometrical theory of diffraction (GTD) [6], [7]; the uniform theory of diffraction (UTD) [8], [9]; or knife-edge diffraction (KED) [10]–[22]. The scope of this paper focuses on KED theory due to its computational simplicity [9].

(Corresponding author: Fahd Nasser Alsaleem).

Fahd Nasser Alsaleem is with the Department of Electrical Engineering, College of Engineering, Qassim University, Unaizah, Saudi Arabia. (e-mail: f.alsaleem@qu.edu.sa).

John S. Thompson, David I. Laurenson, Symon K. Podilchak, and Cristian A Alistarh are with the Institute for Digital Communications (IDCOM) School of Engineering, The University of Edinburgh, Edinburgh EH9 3JL, U.K. (e-mail: john.thompson@ed.ac.uk; Dave.Laurenson@ed.ac.uk; s.podilchak@ed.ac.uk, calistarh@ieee.org).

The METIS channel models [12] came up with a simple numerical approach that models a blocker as a thin screen. This effective blockage model was endorsed by the 3GPP standards body [13]. NYU researchers found this model is less effective when both transmit and receive antennas are directive [14], [15]. To overcome this limitation, they provided a further improvement by considering the directional antenna patterns in the loss calculations.

The European Union H2020-5GPPP project mmMAGIC [18] proposed a blockage model that builds on the 3GPP model. They stated that the 3GPP KED model [13] underestimates the blockage loss since it does not consider the phase differences between the diffracted paths around the blockage screen. Thus, they proposed a modified model that is claimed to be more accurate. It takes into account the fading effect resulting from the summation of the four diffracted paths.

In our initial work [23], we have provided a limited set of blockage loss measurement using a few metal sheets, but cylinder blockers were not considered. Also, the initial work was limited to variants of the 3GPP blockage model which did not consider the phase of diffracted paths behind the blockage screen. The initial work did not investigate the applicability of the mmMAGIC blockage model. Furthermore, the initial work did not investigate the impact of these measured losses on the spectral efficiency (SE) of mmWave in the presence of blockers. All these limitations are addressed in this paper. This paper focuses on investigating the impact of small blockers in both indoor and outdoor environments. We focus on different sizes of metal sheets and cylinders that are small relative to the human body.

The first research question would the mmMAGIC model, which considers the phase variations as well, succeed in capturing the attenuation of small blockers? Secondly, how much can small blockers could affect the mmWave signal, i.e. the received SE? These are investigated in this paper.

The main contributions of this study are as follows:

- Introduce further attenuation measurements for narrow cylinder blockers and different sizes of metal sheets, i.e. in the range of 10 cm up to 33 cm.
- Investigating the applicability and the limitations of the state-of-the-art KED blockage model, the mmMAGIC model, to assess its suitability for small blockers.
- To evaluate small-blockage effects on the received spectral efficiency, we have inserted the measured attenuation profiles of small blockers into an outdoor scenario.

These contributions shed light on how severely the small blockages can affect the mmWave received signal. This study provides a clear understanding of the behavior of the channel attenuation resulting from blockers that are smaller than

human bodies, which can affect the performance of mmWave communication systems [24].

The remainder of this paper is structured into four further sections as follows: Section II presents the three KED approaches of blockage modeling. That is followed by Section III, which introduces the measurement settings. Section IV shows the results and discussions. Finally, the conclusions are in the last section.

II. Blockage Modeling Approaches

The blockage attenuation is added as another loss term to the received power formula of Friis's free-space path loss equation [25] as follows:

$$P_R = P_T - L_{FS} - L_{Blocker} \quad \text{(dB)} \tag{1}$$

where P_R and P_T are the received and the transmit power respectively, while L_{FS} and $L_{Blocker}$ represent the free space path loss and the observed blockage shadowing loss.

In this paper, we compare the measured attenuation resulting from relatively small blockers with the performance of the mmMAGIC blockage model. Also, to show the improvement of the mmMAGIC blockage model in capturing the resulting attenuation of small blockers, the other existing KED blockage models, such as the 3GPP model [13], the version including directional antenna patterns [14], will be used for comparison.

A. Knife-Edge Diffraction and the 3GPP Blockage Model

Based on the knife-edge diffraction (KED) theory, the blocker is assumed to be a thin screen with infinite width and sharp edge. The blockage attenuation is obtained from the superposition of the electric field behind the KED screen. First, let us introduce the Fresnel-Kirchoff parameter v for wavelength λ as follows: $v = \varphi\sqrt{\frac{2d_1d_2}{\lambda(d_1+d_2)}}$ where φ is the diffracted angle and $d1, d2$ are the transmitter and receiver distances to the screen as shown in Fig. 1. The electric strength at the receiver behind the KED screen is obtained by the Fresnel-integral $F(v)$ that sums up all Huygens' secondary sources from v to ∞ which gives the well-known diffraction gain expression as follows [10], [26]:

$$F(v) = \frac{1+\mathrm{j}}{2}\left\{\left[\frac{1}{2} - C(v)\right] - \mathrm{j}\left[\frac{1}{2} - S(v)\right]\right\} \tag{2}$$

where $C(v) - \mathrm{j}S(v) = \int_0^v \exp\left(-\mathrm{j}\frac{\pi}{2}t^2\right) dt$ is the complex Fresnel-integral. However, instead of computing the complex integration to get the loss value, a very efficient approximation is provided by the 3GPP standards body [13].

The 3GPP model renders each blocker as a finite four-edge screen. The diffraction value caused by each edge is obtained by:

$$F = \frac{\operatorname{atan}\left(\pm\frac{\pi}{2}\sqrt{\frac{\pi}{\lambda}\left(D_1 + D_2 - d\right)}\right)}{\pi} \tag{3}$$

where λ is the wavelength, D_1 and D_2 are the projected distance from the TX and RX nodes to the screen, and d is the projected distance between TX and RX nodes, as shown in Fig. 1. The resulting blockage attenuation behind the four-edges screen is computed as follows:

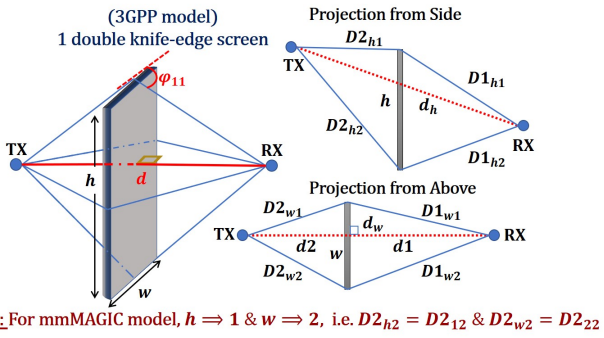

Fig. 1. KED Shadowing screen model: One screen blockage model [13] that represents the following models: 3GPP, 3GPP+antenna gain and mmMAGIC.

$$L_{Blocker} = -20\log_{10}\left(1 - \left(F_{h1} + F_{h2}\right)\left(F_{w1} + F_{w2}\right)\right) \text{ (dB)} \tag{4}$$

where F_{h1}, F_{h2}, F_{w1} and F_{w2} are the four-edge diffraction values; h and w are the height and width of the screen, as shown in Fig. 1.

However, by assuming an infinite screen height, as assumed by several studies in the literature [14], (4) is simplified further as follows:

$$L_{Blocker} = -20\log_{10}\left(1 - \left(F_{w1} + F_{w2}\right)\right) \text{ (dB)} \tag{5}$$

Given that the 3GPP blockage model works better for the omnidirectional antennas [12], using the model for directional antennas would underestimate the blockage attenuation by up to 10-20 dB [14]. Thus, the NYU research group have modified the loss equation (5) to include the corresponding linear antenna gain [14] as follows:

$$L_{Blocker} = -20\log_{10}\left|\left(\frac{1}{2} - F_{w1}\right)\cdot\sqrt{G_{D2_{w1}}}\cdot\sqrt{G_{D1_{w1}}} + \left(\frac{1}{2} - F_{w2}\right)\cdot\sqrt{G_{D2_{w2}}}\cdot\sqrt{G_{D1_{w2}}}\right| \text{ (dB)} \tag{6}$$

where $G_x, (x = D2_{w1}, D1_{w1}, D2_{w2}, D1_{w2})$, are the normalized linear gains of the directional antennas relative to the normalized boresight gain defined as $G(0) = 1$.

In our initial work [23], we have shown that considering the antenna gain would significantly improve the 3GPP model only if the blocker completely blocks the main beam of the directional antenna pattern. Otherwise, considering the antenna gain shows just a slight improvement of 2-3 dB in model accuracy. Our results show significant differences between measured and model results so there is a need for an improved version of the 3GPP blockage model. It is essential to have a model that considers the phase differences of the diffracted paths around the blocker, which leads us to the mmMAGIC blockage model.

B. The mmMAGIC Blockage Model:

The 3GPP model does not consider the phase variations between the diffracted paths behind the screen, which makes

the 3GPP model underestimate the blockage attenuation. Thus, in [18], they have introduced some new parameters to the loss calculation equation to account for the phase variations. These are: ph_{ij}, Ph and $\cos\varphi_{ij}$. For the mmMAGIC model, the loss is computed as follows:

$$L_{Blocker} = -20\log_{10}\left(1 - \prod_{i=1}^{2}\sum_{j=1}^{2} s_{ij}\left[\frac{1}{2} - \frac{ph_{ij}}{Ph}F_{ij}\right]\right) \text{ (dB)} \tag{7}$$

where s_{ij} is the sign term, which is $s_{ij} = 1$ if NLOS. If LOS, $s_{ij} = \text{sgn}\ (D1_{ij} + D2_{ij} - D1_{ik} - D2_{ik})$, where sgn(.) is a function that specifies the sign of the argument. The scalar k = mod$(j, 2)+1$. The remaining variables are defined as follows:

$$F_{ij} = \cos\varphi_{ij}\left[\frac{1}{2} - \frac{1}{\pi}\tan^{-1}\left(\frac{V_{ij}\pi}{2}\right)\right] \tag{8}$$

$$ph_{ij} = \exp\left[\frac{-\text{j}2\pi}{\lambda}\left(D1_{ij} + D2_{ij}\right)\right] \tag{9}$$

$$Ph = \exp\left[\frac{-\text{j}2\pi d}{\lambda}\right] \tag{10}$$

$$V_{ij} = \sqrt{\frac{\pi}{\lambda}\left(D1_{ij}{}^{\text{proj}} + D2_{ij}{}^{\text{proj}} - d_i{}^{\text{proj}}\right)} \tag{11}$$

The variable $\cos\varphi_{ij}$ in (8) considers the increase of diffraction loss in the shadow zone behind the blockage screen. By assuming the values of the new parameters: ph_{ij}, Ph and $\cos\varphi_{ij}$ are one, we simplify to the 3GPP blockage loss equation, i.e. (4).

III. Measurement Settings

This study investigates the blockage effect within critical Tx-Rx distance ranges, where a small blocker could significantly affect the radiated main beam. For a system with a center carrier frequency of 28 GHz, the critical TX-RX distance is few meters. It only has a significant effect at short distances when the blocker occupies a large proportion of the main beam or first Fresnel zone area. For larger TX-RX distances, the blocker would normally have a negligible effect due to its small size. We have two directional horn transmit and receive antennas are placed at the two ends of an anechoic chamber, with a 2 m TX-RX distance. To minimize any measurement uncertainty, we have performed a calibration before starting taking the measurements of the S21 parameter. We measure the received power without the presence of the blocker and with the path-loss; then, we have measured the received power in the presence of the blocker. The relative power measurement is just the difference of these two values.The far-field zone starts from around $\geq \frac{2D^2}{\lambda}$= 0.35 m $\approx 35\lambda$ [27], for the used the center carrier frequency, which is 28 GHz. The transmit power is -10 dBm. We move the blocker by small steps to cross, in the middle, the LOS path between the two antennas; the crossing point is 1 m distant from each antenna. Table I shows the measurement settings.

A. Blockers Types and Sizes

Most road signs are metal sheets of different sizes, and their holding posts usually are either metal or strong-plastic cylinders. In this paper, five blockers were used, as follows:

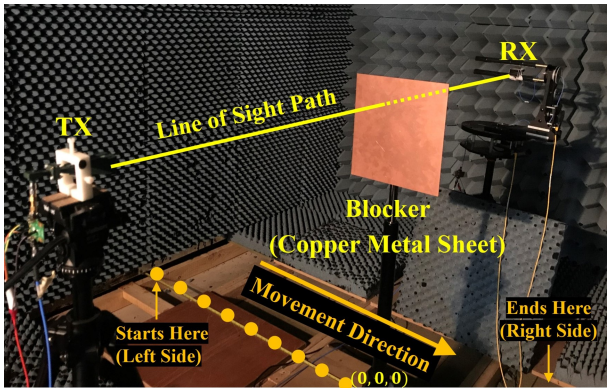

Fig. 2. The rectangular metal sheet blocking the LOS in the anechoic chamber.

TABLE I
Lab Measurement Settings

Transmit Power	-10 (dBm)
TX-RX Distance	2 (m)
Antenna Type	20 (dBi) Horn Antenna series 240 from Flan Microwave
Transmitter Amplifier	from Analog Devices, with the Hittite 123813-1 evaluation board
Antenna Dimensions	3.5 x 2.5 (cm)
Chamber Dimensions	2.67 x 5 x 2.34 (m)
Height of TX, RX and Blocker	1 (m)
Carrier Frequency	27, 28, 29 (GHz)
Spectrum Analyzer	Keysight N9030B PXA
Sample Space	1 (cm) $\approx \lambda$
TX/RX Azimuth and Elev. (HPBW)	20.46°
Performance Metric: Relative Power [12], [16]	A calibration process is implemented to remove free space path loss - results show only the gain of the blocker on the signal.
Blocker's Dimensions (Width x Height)	
1- Small Square $BL(1)$	16.5 x 16.5 (cm)
2- Rectangular $BL(2)$	28.2 x 36 (cm)
3- Large Square $BL(3)$	33 x 33 (cm)
4- Cylinder $BL(4)$ and $BL(5)$	r_{BL}=5.7, h=141, thick. of 0.45(cm)

1) Metal sheet blocker:
   a) ***BL(1)***: Small square sheet - size:(16.5×16.5) cm.
   b) ***BL(2)***: Rectangular sheet - size: (36×28.2) cm.
   c) ***BL(3)***: Large square sheet - size: (33×33) cm.
2) Cylinder Blocker: the dimensions are: radius 5.7 cm, height 141 cm and thickness 4.5 mm.
   a) ***BL(4)***: PVC Plastic cylinder.
   b) ***BL(5)***: Metallic cylinder: PVC plastic cylinder wrapped with thick aluminium foil.

IV. Results and Discussions

The results in this section are divided into two main parts. First, we apply the enhanced KED simulation blockage model, mmMAGIC, to each scenario of the five measured blockers. In the second part of the results, we show how the attenuation profiles can be incorporated in mmWave spectral efficiency results for an outdoor scenario.

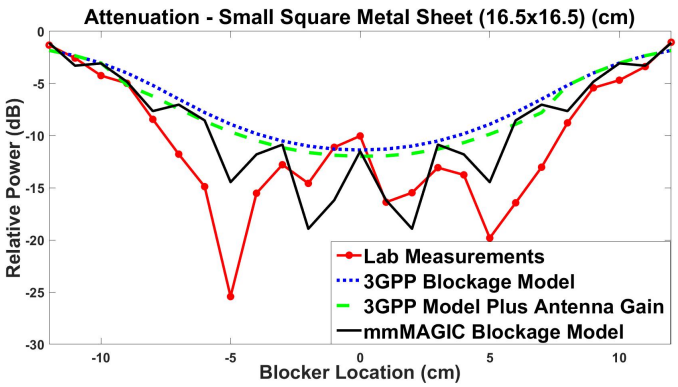

Fig. 3. The attenuation of BL(1): (16.5 cm by 16.5 cm) metal sheet. Comparison between measurements and the following models: a) 3GPP eq. (5), b) 3GPP (including the antenna gain) eq. (6), c) mmMAGIC eq. (7). The center carrier frequency is 28 GHz.

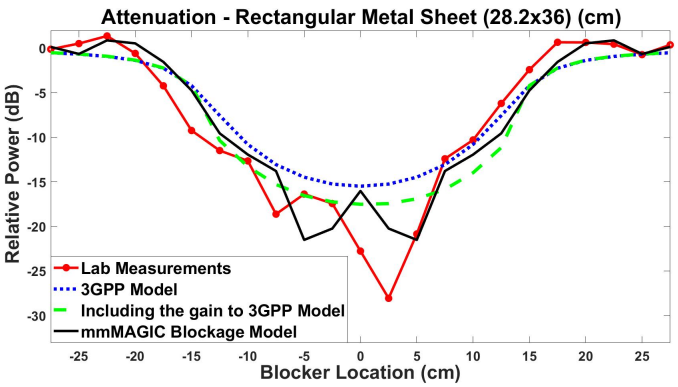

Fig. 4. The attenuation of BL(2): (36 cm by 28.2 cm) metal sheet. Comparison between measurements and these models: a) 3GPP eq. (5), b) 3GPP (including the antenna gain) eq. (6), c) mmMAGIC eq. (7). The carrier frequency is 28 GHz.

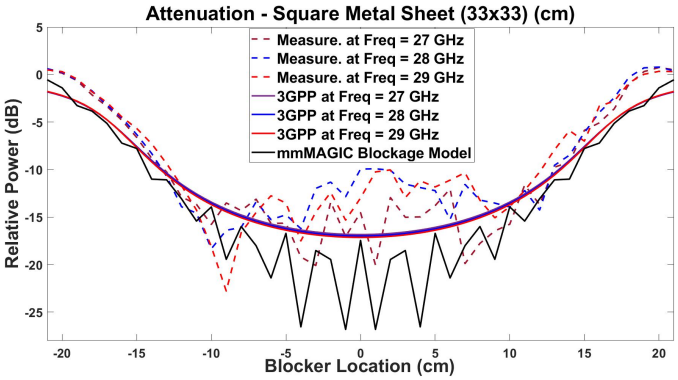

Fig. 5. The attenuation of BL(3): (33 cm by 33 cm) metal sheet for three different frequencies. Comparison between measurements and the following models: a) 3GPP eq. (5) and b) mmMAGIC eq. (7). The center carrier frequency is 27-29 GHz.

A. *Part 1 Results: Attenuation of the 5 Small Blockers*

In the following subsections, we present the measured attenuation caused by each one of the five blockers, i.e. $BL(1)$-$BL(5)$. For each blocker, we apply all the three KED blockage simulation models: a) 3GPP eq. (5), b) 3GPP + including the gain eq. (6), c) mmMAGIC eq. (7). It should be mentioned that the measurement settings were the same for all blockers. Each blocker is moved from the left side of the anechoic chamber to the right side perpendicularly crossing the LOS in the middle between the two antennas, i.e., 1 m from each antenna, as shown in Fig. 2. The distance between each measurement is 1 cm $\approx \lambda|_{f_c=28\text{GHz}}$. All figures show the relative power values due to blockage only with no other attenuation effects, i.e., removing the path loss effect, as in [12], [16].

*1) **Attenuation of BL(1): (16.5×16.5) cm metal sheet:***

Fig. 3 shows that the 3GPP model fails to estimate the two troughs with around 20 dB difference in relative power. As discussed earlier, including the antenna gain into the calculations does not help. However, the mmMAGIC blockage model has an advantage over the 3GPP model since it accounts for the fast-fading resulting from summing the diffracted paths. The mmMAGIC curve performs closer to the measured attenuation and follows the same fluctuation trend, but it slightly mismatches the main two attenuation peaks at (+/- 5) cm locations. However, both 3GPP and mmMAGIC models use two or four ray approximations of the exact diffraction pattern; so both are simplifications of the actual diffraction patterns all around the blocker, which could explain the mismatch. Nevertheless, the mmMAGIC model shows a better performance than the 3GPP in capturing the measured attenuation curve; this is due to the fact it considers the phase of the reflected paths.

*2) **Attenuation of BL(2): (36×28.2) cm metal sheet:***

For a wider blocker case, Fig. 4 shows the measured attenuation caused by a rectangular metal sheet. The 3GPP model underestimates the measured attenuation curve, with a gap of $\approx$ 13 dB. Including the antenna gain enhances the 3GPP performance further, by only 2 or 3 dB. Both scenarios do not capture the fluctuations. However, the mmMAGIC model shows better behavior by following the trend of the measured curve, but it underestimates the highest attenuation peak around the middle at the +2.5 cm location.

*3) **Attenuation of BL(3): (33×33) cm metal sheet:***

The blocker sheet is now about 30λ wide, Fig. 5 shows that the 3GPP model (4) successfully fits the measurements curve for three different center carrier frequency. The 3GPP simulation results do not show a significant change after increasing the center carrier frequency by 2 GHz (i.e. from 27 GHz to 29 GHz). The measurement results show again some fluctuations, which are again not captured due to the limitations of the 3GPP model. For the center carrier frequency of 28 GH, the mmMAGIC model has a fluctuation trend that shows similar behavior to the measured curve, but it slightly overestimates the measured attenuation.

*4) **Attenuation of BL(4): The Plastic Cylinder:***

The cylinder blocker has a more complex structure in comparison to the metal sheet blockers. The cylinder diameter is 11.4 cm which means a narrower width than the width of all the previous metal sheet blockers. We have two scenarios for the cylinder blocker: a PVC plastic cylinder and a metalic cylinder where the plastic one is wrapped in aluminum foil.

In Fig. 6, the measurements show a W-shaped curve, where the attenuation in the middle is close to zero, and it peaks when the blocker is moved to either side. One possible

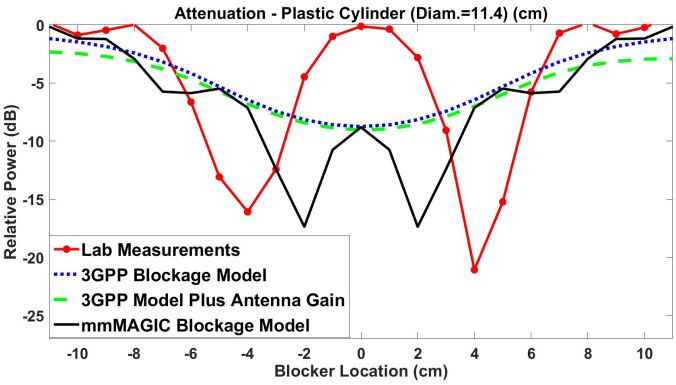

Fig. 6. The attenuation of BL(4)- the plastic cylinder. Comparison between measurements and these models: a)3GPP eq. (5), b) 3GPP (including the antenna gain) eq. (6), c)mmMAGIC eq. (7). Center carrier freq. is 28 GHz.

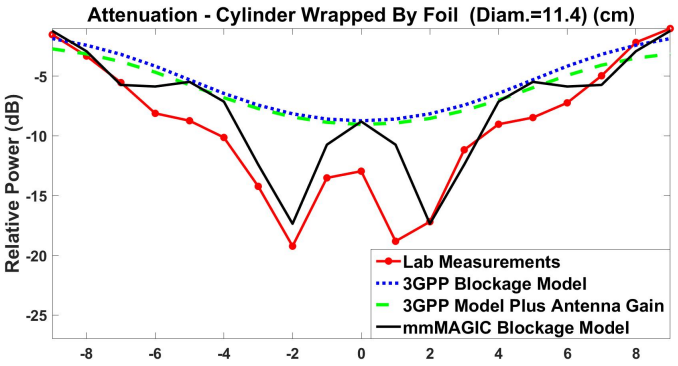

Fig. 7. The attenuation of BL(5): the metallic cylinder. Comparison between measurements and the following models: a) 3GPP eq. (5), b) 3GPP (including the antenna gain) eq. (6), c) mmMAGIC eq. (7). The center carrier frequency is 28 GHz.

justification for this is that the diffracted rays around the two vertical sides of the plastic cylinder are adding constructively, so they give the maximum value in the middle where the constructive interference of the two diffracted waves occurs. The 3GPP blockage model fails to match the measurements. Also, including the antenna gain in the loss calculation of the 3GPP blockage does not show any significant improvement. However, the mmMAGIC blockage model considers the phase of the reflected paths, which is its advantage over the 3GPP model. Although the mmMAGIC model shows the same behavior as the measured curve, the peaks do not match well. However, as stated in [28], due to the shape of the cylinder blocker, the KED model may not accurately capture the loss since it is based on a sharp edge assumption, not a curved surface. Using a creeping wave linear model, as in [29], [30], may result in a better fit with the measured loss.

*5) **Attenuation of BL(5): The Metallic Cylinder:***

Fig. 7 shows the attenuation caused by the cylinder wrapped in aluminum foil. The measured curve has a W-shape, where the attenuation in the middle is around -15 dB, while it reaches -20 dB when the blocker is moved to either side. The behavior of our measurements here is consistent with the measurements of [7], who used a metal cylinder to model the attenuation caused by a human leg in the 60 GHz carrier frequency band. Both the 3GPP model with and without the antenna gain included in the loss computation underestimates the measured loss. The best model here is the mmMAGIC model, which has a good fit with the measured curve.

Discussion: From all the above results, clearly that the 3GPP blockage model does not work well in replicating the measured attenuation for the narrow-width blockers, i.e., in the range of $10-20\lambda$. Also, even including the antenna gain into the 3GPP blockage calculations does not show any significant improvement. On the other hand, the mmMAGIC model that accounts for the fast-fading behind the blocker generally performs a good fit with the measured loss for narrow-width blockers. Unlike the 3GPP model, the mmMAGIC model mimics the fluctuation resulting from the phase differences between the four diffracted paths behind the blocker. Table II shows that varying the carrier frequency by (+/- 1 GHz) does not affect the attenuation values significantly.

TABLE II
FREQUENCY COMPARISON BASED ON THE MEAN VALUE OF THE MEASURED ATTENUATION FOR ALL BLOCKAGE MODELS.

Mean Blockage Attenuation (dB)			
Blocker Type	Central Frequency		
	27 GHz	28 GHz	29 GHz
$BL(1)$**:Small Square**	-13.27	-14.12	-14.62
$BL(2)$**:Rectangular**	-17.76	-17.75	-16.6
$BL(3)$**:Large Square**	-14.71	-12.88	-12.83
$BL(4)$**:Plastic Cylinder**	-6.59	-6.17	-5.66
$BL(5)$**:Metallic Cylinder**	-12.47	-12.77	-12.45

B. Part 2 Results: Blocker effects on the Spectral Efficiency

In this part, the paper's focus moves to show how the measured attenuations are used in computer simulations for an overall system evaluation of mmWave in the presence of blockers. We have created a simple outdoor scenario for a moving transceiver passing by a basestation in the presence of blockers. An arbitrary attenuation function has been applied randomly at different locations by using a two state Markov chain blocking function [31]. In the following result, two out of the five blocker attenuation profiles provided in this paper have been used. These blockers are $BL(3)$: the 33-by-33 cm square metal sheet, and $BL(5)$: the metallic cylinder. Most road-signs have similar shapes to these blockers.

Fig. 8 shows the received spectral efficiency (SE) of 200 sample points within a two-meter sector of the transceiver movement. We have plotted three curves: 1- The green dotted curve that shows the received SE when there is no blocker at all. 2- The red curve which represents the received SE including the blocker effect. The attenuation is taken from the measurements of this paper. 3- The blue dashed curve represents the received SE with blockers effect, but the blockers are from the simulation models rather than the measurements. For blocker $BL(3)$, we choose the best fit simulation blockage model which is the 3GPP model, while for $BL(5)$ blocker, we applied the mmMAGIC model. From these curves, we conclude two points: 1- even small blockers could affect the signal significantly and reduce the received SE by around 6-7 bits/s/Hz. 2- the simulation models (i.e. the blue curves) could be used instead of the measured attenuation (i.e. the red curve) since they show a similar performance.

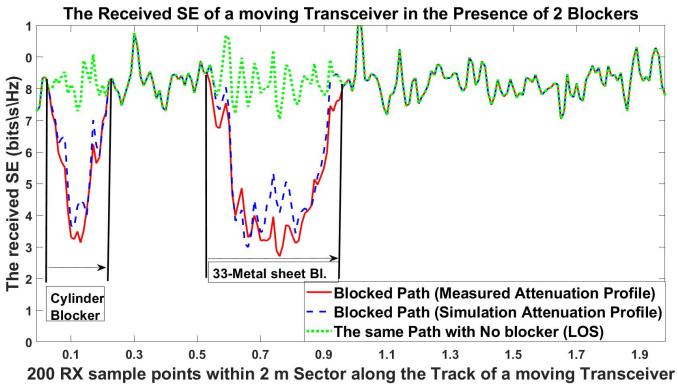

Fig. 8. The received SE (1 run) at a sector of the RX track in the presence of two blocker-types: $BL(3)$ and $BL(5)$. The red curves represent the lab-measured attenuation of the blockers while the blue curves are the simulated attenuation (3GPP for $BL(3)$ and mmMAGIC for $BL(5)$).

V. Conclusions

We have shown that the relatively narrow-width blockers, i.e., in the range of 10-33 cm., attenuate the mmWave signals by 10-30 dB. Given that the 3GPP blockage model underestimates the measured attenuation of these blockers by 10 dB, we have adopted the mmMAGIC blockage model, which has the advantage over the 3GPP model of considering the phase of the diffracted paths behind the blocker. The curve of the mmMAGIC blockage model, in general, performs closely to the measured attenuation. Moreover, the spectral efficiency results of the mmWave system show that even a small-size blocker attenuates the received signal by 6-7 bits/s/Hz.

References

[1] C. Seker, M. T. Güneser, and T. Ozturk, "A review of millimeter wave communication for 5G," in *2018 2nd International Symposium on Multidisciplinary Studies and Innovative Technologies (ISMSIT)*, October 2018, pp. 1–5.

[2] M. K. Samimi and T. S. Rappaport, "3-D millimeter-wave statistical channel model for 5G wireless system design," *IEEE Transactions on Microwave Theory and Techniques*, vol. 64, no. 7, pp. 2207–2225, 2016.

[3] S. Sun, G. R. MacCartney, M. K. Samimi, and T. S. Rappaport, "Synthesizing omnidirectional antenna patterns, received power and path loss from directional antennas for 5G millimeter-wave communications," in *2015 IEEE Global Communications Conference (GLOBECOM)*, December 2015, pp. 1–7.

[4] S. Sun, T. S. Rappaport, R. W. Heath, A. Nix, and S. Rangan, "MIMO for millimeter-wave wireless communications: beamforming, spatial multiplexing, or both?" *IEEE Communications Magazine*, vol. 52, no. 12, pp. 110–121, 2014.

[5] J. S. Lu, D. Steinbach, P. Cabrol, and P. Pietraski, "Modeling human blockers in millimeter wave radio links," *ZTE communications*, vol. 10, no. 4, pp. 23–28, 2012.

[6] W. Qi *et al.*, "Measurements and modeling of human blockage effects for multiple millimeter wave bands," in *2017 13th International Wireless Communications and Mobile Computing Conference (IWCMC)*, June 2017, pp. 1604–1609.

[7] C. Gustafson and F. Tufvesson, "Characterization of 60 GHz shadowing by human bodies and simple phantoms," in *2012 6th European Conference on Antennas and Propagation (EUCAP)*, March 2012, pp. 473–477.

[8] A. G. Aguilar, P. H. Pathak, and M. Sierra-Pérez, "A canonical UTD solution for electromagnetic scattering by an electrically large impedance circular cylinder illuminated by an obliquely incident plane wave," *IEEE Transactions on Antennas and Propagation*, vol. 61, no. 10, pp. 5144–5154, October 2013.

[9] M. Jacob *et al.*, "Fundamental analyses of 60 GHz human blockage," in *2013 7th European Conference on Antennas and Propagation (EuCAP)*, April 2013, pp. 117–121.

[10] J. Kunisch and J. Pamp, "Ultra-wideband double vertical knife-edge model for obstruction of a ray by a person," in *2008 IEEE International Conference on Ultra-Wideband*, vol. 2, September 2008, pp. 17–20.

[11] J. Medbo and F. Harrysson, "Channel modeling for the stationary UE scenario," in *2013 7th European Conference on Antennas and Propagation (EuCAP)*, April 2013, pp. 2811–2815.

[12] V. Nurmela, A. Karttunen, A. Roivainen, L. Raschkowski, V. Hovinen, J. Y. EB, N. Omaki, K. Kusume, A. Hekkala, R. Weiler *et al.*, "Deliverable D1. 4 METIS channel models," in *Proc. Mobile Wireless Commun. Enablers Inf. Soc.(METIS)*, 2015, p. 1.

[13] "Study on channel model for frequency spectrum above 6 GHz (release 14)," *Technical Report TR 38.900, 3GPP*, 2017.

[14] G. R. MacCartney *et al.*, "Millimeter-wave human blockage at 73 GHz with a simple double knife-edge diffraction model and extension for directional antennas," in *2016 IEEE 84th Vehicular Technology Conference (VTC-Fall)*, September 2016, pp. 1–6.

[15] G. R. MacCartney *et al.*, "Millimeter-wave base station diversity and human blockage in dense urban environments for coordinated multipoint (CoMP)," NYU Tandon School of Engineering, NYU WIRELESS, NYU Tandon School of Engineering, 2 MetroTech Center, Brooklyn, NY 11201, Tech. Rep. NYU WIRELESS TR 2018-002, May 2018.

[16] M.Jacob *et al.*, "A ray tracing based stochastic human blockage model for the IEEE 802.11ad 60 GHz channel model," in *Proceedings of the 5th European Conference on Antennas and Propagation (EUCAP)*, April 2011, pp. 3084–3088.

[17] M. Jacob *et al.*, "Extension and validation of the IEEE 802.11ad 60 GHz human blockage model," in *2013 7th European Conference on Antennas and Propagation (EuCAP)*, April 2013, pp. 2806–2810.

[18] M. Peter *et al.*, "Measurement results and final mmMAGIC channel models," *Deliverable D2*, vol. 2, p. 12, 2017. [Online]. Available: $https://bscw.5g-mmmagic.eu/pub/bscw.cgi/d202656/mmMAGIC_D2-2.pdf$

[19] N. Tran, T. Imai, and Y. Okumura, "Study on characteristics of human body shadowing in high frequency bands: Radio wave propagation technology for future radio access and mobile optical networks," in *2014 IEEE 80th Vehicular Technology Conference (VTC2014-Fall)*, 2014, pp. 1–5.

[20] X. Chen, L. Tian, P. Tang, and J. Zhang, "Modelling of human body shadowing based on 28 GHz indoor measurement results," in *2016 IEEE 84th Vehicular Technology Conference (VTC-Fall)*, 2016, pp. 1–5.

[21] V. Raghavan, L. Akhoondzadeh-Asl, V. Podshivalov, J. Hulten, M. A. Tassoudji, O. H. Koymen, A. Sampath, and J. Li, "Statistical blockage modeling and robustness of beamforming in millimeter-wave systems," *IEEE Transactions on Microwave Theory and Techniques*, vol. 67, no. 7, pp. 3010–3024, 2019.

[22] V. Raghavan, S. Noimanivone, S. K. Rho, B. Farin, P. Connor, R. A. Motos, Y.-C. Ou, K. Ravid, M. A. Tassoudji, O. H. Koymen, and J. Li, "Hand and body blockage measurements with form-factor user equipment at 28 ghz," 2019.

[23] F. Alsaleem, J. S. Thompson, D. I. Laurenson, S. K. Podilchak, and C. A. Alistarh, "Small-size blockage measurements and modelling for mmWave communications systems," in *2020 IEEE 31st Annual International Symposium on Personal, Indoor and Mobile Radio Communications (PIMRC)*, 2020.

[24] C. Slezak *et al.*, "Empirical effects of dynamic human-body blockage in 60 GHz communications," *IEEE Communications Magazine*, vol. 56, no. 12, pp. 60–66, December 2018.

[25] D. C. Hogg, "Fun with the Friis free-space transmission formula," *IEEE Antennas and Propagation Mag.*, vol. 35, no. 4, pp. 33–35, 1993.

[26] E. C. Jordan and K. G. Balmain, "Electromagnetic waves and radiating systems," 1968.

[27] Everything RF. [Online]. Available: https://www.everythingrf.com/rf-calculators/antenna-near-field-distance-calculator

[28] T. S. Rappaport, G. R. MacCartney, S. Sun, H. Yan, and S. Deng, "Small-scale, local area, and transitional millimeter wave propagation for 5G communications," *IEEE Transactions on Antennas and Propagation*, vol. 65, no. 12, pp. 6474–6490, 2017.

[29] T. Mavridis, L. Petrillo, J. Sarrazin, D. Lautru, A. Benlarbi-Delaï, and P. De Doncker, "Creeping wave model of diffraction of an obliquely incident plane wave by a circular cylinder at 60 GHz," *IEEE Transactions on Antennas and Propagation*, vol. 62, no. 3, pp. 1372–1377, 2014.

[30] L. Piazzi and H. L. Bertoni, "Effect of terrain on path loss in urban environments for wireless applications," *IEEE Transactions on Antennas and Propagation*, vol. 46, no. 8, pp. 1138–1147, 1998.

[31] F. Alsaleem, J. S. Thompson, and D. I. Laurenson, "Adaptive sum of markov chains for modeling 3D blockage in mmWave V2I communications," *IEEE Transactions on Vehicular Technology*, 2020.